JOM, Vol. 67, No. 4, 2015
DOI: 10.1007/s11837-015-1350-7

Chimeric Peptides as Implant Functionalization Agents for Titanium Alloy Implants with Antimicrobial Properties

DENIZ T. YUCESOY,[1] MARKETA HNILOVA,[1] KYLE BOONE,[2] PAUL M. ARNOLD,[3] MALCOLM L. SNEAD,[4] and CANDAN TAMERLER[5,6]

1.—Department of Materials Science and Engineering, GEMSEC, Genetically Engineered Materials Science and Engineering Center, University of Washington, Seattle, WA 98195, USA. 2.—Bioengineering Program and Bioengineering Research Center, University of Kansas, Lawrence, KS 66045, USA. 3.—Department of Neurosurgery, School of Medicine, Spinal Cord Injury Center, University of Kansas, Kansas City, KS 66160, USA. 4.—Ostrow School of Dentistry of USC, Center for Craniofacial Molecular Biology, University of Southern California, Los Angeles, CA 90032, USA. 5.—Department of Mechanical Engineering & Bioengineering Research Center, University of Kansas, Lawrence, KS 66045, USA. 6.—e-mail: ctamerler@ku.edu

Implant-associated infections can have severe effects on the longevity of implant devices and they also represent a major cause of implant failures. Treating these infections associated with implants by antibiotics is not always an effective strategy due to poor penetration rates of antibiotics into biofilms. Additionally, emerging antibiotic resistance poses serious concerns. There is an urge to develop effective antibacterial surfaces that prevent bacterial adhesion and proliferation. A novel class of bacterial therapeutic agents, known as antimicrobial peptides (AMPs), are receiving increasing attention as an unconventional option to treat septic infection, partly due to their capacity to stimulate innate immune responses and for the difficulty of microorganisms to develop resistance towards them. While host and bacterial cells compete in determining the ultimate fate of the implant, functionalization of implant surfaces with AMPs can shift the balance and prevent implant infections. In the present study, we developed a novel chimeric peptide to functionalize the implant material surface. The chimeric peptide simultaneously presents two functionalities, with one domain binding to a titanium alloy implant surface through a titanium-binding domain while the other domain displays an antimicrobial property. This approach gains strength through control over the bio-material interfaces, a property built upon molecular recognition and self-assembly through a titanium alloy binding domain in the chimeric peptide. The efficiency of chimeric peptide both in-solution and absorbed onto titanium alloy surface was evaluated *in vitro* against three common human host infectious bacteria, *Streptococcus mutans*, *Staphylococcus epidermidis*, and *Escherichia coli*. In biological interactions such as occur on implants, it is the surface and the interface that dictate the ultimate outcome. Controlling the implant surface by creating an interface composed chimeric peptides may therefore open up new possibilities to modify the implant site and tailor it to a desirable bioactivity.

INTRODUCTION

Titanium and its alloys have been extensively used in orthopedic and dental implants, mainly due to their unique combination of excellent mechanical properties, corrosion resistance, biocompatibility and osseointegration.[1–5] However, the risk of failure of these implants, which can lead to suboptimal clinical outcomes, still poses a significant threat to patients and post-surgical challenges to their clinicians.[6,7] Although recent enhancements in the design of prosthetic devices and the advancements in surgical procedures have reduced the number of complications leading to failure, implant associated

(Published online March 7, 2015)

bacterial infections is still a serious challenge and a major cause of post-surgical morbidity and mortality.[8]

Implant materials provides an ideal surface to the growth of common pathogens such as *Staphylococcus aureus*, *Staphylococcus epidermidis*, and *Pseudomonas aeruginosa*, which could be acquired shortly after surgery or at a later date. Failure to adequately combat these bacterial infections at the implant-tissue interface often results in complex revision procedures, with an economic burden to the health-care system, and in most cases the removal of the implant with the re-instrumentation at a later date is the only remedy. Moreover, formation by these pathogens of complex biofilm structures on the implant surface or its periphery can make the problem more difficult to address. Bacterial biofilm formed on the implant creates a barrier that decreases penetration of antimicrobial agents reducing the susceptibility of the biofilms members to drug delivery.[6,9,10] Even with substantial interest and efforts to improve local delivery of systemic antibiotics to implant surfaces, challenges regarding diluted drug levels at the target site and the potential toxicity of conventional antibiotics still need to be addressed.[11,12] Furthermore, the potential development and spread of antibiotic-resistant pathogens such as the methicillin-resistant *S. aureus* (MRSA) remain a challenge to hospital acquired infections.[10,13]

One of the successful survival strategies of bacteria is their ability to adhere to virtually any surfaces through their various types of adhesins. Free-floating bacteria can activate the biofilm-related phenotype after their attachment to implant surfaces. The initial phase of their attachment is relatively less stable compared to later stages where bacteria start expressing biofilm-specific genes. The window of opportunity relies on designing the surfaces prior to bacterial attachment moving into almost an irreversible phase, where the biofilm formation starts. Development of implant surfaces that would prevent bacterial adhesion becomes critical. Several surface coating and functionalization strategies have been reported to overcome implant failure associated with infections. In an attempt to render the implant surface non-adhesive and/or to introduce antimicrobial surfaces, the use of polyethylene glycol (PEG) and its derivatives,[14,15] coatings of albumin,[16] covalent attachment of conventional antibiotics,[17–20] chlorhexidine,[21] silver, nitrogen oxide[22,23] and quaternary ammonia compounds[19,24] have been used. While the activation of implant surfaces by these agents have been shown to reduce bacterial adhesion, existing covalent coupling strategies often require complex chemistry to execute, with the unwieldy requirement of specific functional groups on the surface with extensive optimization steps. Moreover, the limited capacity of this chemical derivatization used for modification of different implant materials makes them far from providing a comprehensive solution.[25–27] Additionally, the slow release of derivatized antimicrobial agents from preloaded implant devices raises concern about a possible link to increased incidences of bacterial resistance and cytotoxicity.[28]

Bioactivation of implant surfaces with more biocompatible and nontoxic biomolecules such as antimicrobial peptides (AMPs) would be a feasible approach to overcome infection derived implant failure without evoking either toxicity or antibiotic resistance. These short, cationic AMPs are evolutionary conserved constituents of the innate immune defense systems of many organisms, including insects, plants, animals and humans.[29–31] AMPs are believed to specifically target and disrupt the integrity of negatively charged cell membrane of microorganisms. Although there is no consensus in their sequence and structure, AMPs usually have an amphipathic structure which serves as efficient ionic recognition between the cationic residues of peptide and the phospholipids of the bacterial membrane.[32,33] Furthermore, in contrast to conventional antibiotics, it is extremely difficult for microorganisms to develop resistance against these peptides because of their highly sophisticated reaction mechanisms and considerably rapid rate action.[29,34] More importantly, AMPs have broad-spectrum antimicrobial activity against gram-positive and gram-negative bacteria, fungi and viruses. AMPs can work synergistically with conventional antibiotics and facilitate antibiotic penetration to the infection site, thus enabling more aggressive biofilm treatment.[29] It has also been demonstrated that the sequence and/or resulting structure of natural AMPs can be utilized as templates for the design of synthetic variants with enhanced antimicrobial activities.[35–37] By retaining their localized effect through tethering and assembly of AMPs as an antimicrobial coating to implant surfaces agents, it could greatly increase effectiveness while reducing potential cytotoxic consequences and collateral damage through vascular redistribution.[38]

Unlike other approaches utilizing covalent linkages to tether AMPs on the implant surface, we have created bifunctional chimeric peptides composed of an implant surface binding peptide and an AMP agent. These bifunctional chimeric peptides rely on the properties of the solid-binding peptides[39] that preferentially bind to the titanium surface, a common implant surface, while freely exposing the AMP motif to combat invading bacteria. This interface on the implant surface is constructed by combining combinatorially selected solid-binding peptides with AMP sequences in different combinations through an intervening flexible linker.[40–44] These bifunctional chimeric peptides were characterized in terms of their binding properties to the titanium surface and their antimicrobial efficacy either in solution or immobilized on the surface. Keeping in mind the importance of assessing any

therapeutic target against a range of problematic bacteria due to varying responses, we chose three different types of bacteria, *Streptococcus mutans, S. epidermidis, and Escherichia coli* to test the efficacy of our bifunctional chimeric peptides against. *S. mutans* is a Gram-positive, biofilm-forming bacterium commonly found in oral implant infections.[45] *S. epidermidis* is a Gram-positive, biofilm-forming bacterium commonly found in orthopedic implant infections, making up 32% of clinical isolates from orthopedic implant infections. *E. coli* is a Gram-negative, slime-producing bacterium occasionally found in orthopedic implant infections.[46,47]

Here, we provide details on an alternative method of implant surface functionalization that does not require complex procedures or the covalent modification of the implant surface.[47–49] The principles laid out in the paper can be applied to other identified AMP sequences, and expanded to a wide range of biomaterials other than titanium by deploying different solid-binding sequences that binds to other biomaterials.[40,49,50] In addition, the structure–function relationships found in this paper can be applied for control of performance over designing chimeric peptides by following emergent rules.[51]

MATERIALS AND METHODS

Target Implant Material Characterization and Preparation

Surface properties of titanium grade V powder (Sigma-Aldrich, St Louis, MO, USA) and titanium grade V implant (Vetimplants, St. Augustine, FL, USA) were determined by scanning electron microscopy (SEM). Elemental composition of the substrate was analyzed by collecting energy-dispersive x-ray spectroscopy (EDS) spectra for 100 s at 9 keV using a LaB_6 filament. Titanium grade V implant (Vetimplants) was cut into approximately 1 cm × 1 cm squares and sharp edges were removed by hand polishing with a 600-grit finish silicon carbide metallurgical paper. Before experimental use, titanium grade V powder and implant pieces were cleaned by sonicating sequentially in a 1:1 acetone:methanol mixture, then isopropyl alcohol, and finally de-ionized water. Then, substrates were sterilized for 15 min under UV light.

Selection of Titanium Binding and Antimicrobial Binding Peptides

Titanium binding peptides (TiBP) were selected by cell surface display[50] and phage display methods. Briefly, for the cell surface display approach, the FliTrx bacterial cell surface display system (Invitrogen, Carlsbad, CA, USA) was used to select peptide sequences against titanium substrates.[52–54] After four rounds of successful biopanning enrichment, the DNA sequences for each of the 60 isolated clones were analyzed. Binding properties for each peptide were characterized by quantitative fluorescent microscopy, employing a Nikon Eclipse TE-2000U fluorescent microscope (Nikon, Melville, NY, USA) equipped with a Hamamatsu ORCA-ER cooled CCD camera (Hamamatsu, Bridgewater, NJ, USA), imaged using a FITC filter (exciter 460–500 nm, dichroic 505 nm, emitter 510–560 nm) and MetaMorph imaging system (Universal Imaging, West Chester, PA, USA). Finally, the binding affinity for each peptide was calculated by determining, in triplicate samples, the average number of adherent bacterial cells expressing the peptide identified on the titanium surface. Consequent on this analysis, the TiBP were grouped as strong, moderate or weak binders, according to their binding capacity.

In the phage display method, the Ph.D.-12 phage display peptide library kit (New England Biolabs, Ipswich, MA, USA) containing 1.2×10^9 different randomized peptide sequences was used as previously described.[55] The peptide library is incubated with titanium grade V powder in potassium carbonate (PC) buffer containing 0.1% Tween 20 detergent (Merck, Whitehouse Station, NJ, USA) and then the unbound phages are removed by washing the surface with PC buffer containing 0.1% detergent (Tween 20 and Tween 80). The bound phages were eluted specifically from the surface using the elution buffer; and the eluted pool was amplified in *E. coli* ER2738. Amplified phages were purified and subsequently used for additional panning rounds. After each round, the phages were grown on solid media, and single clones selected by picking single-phage plaques that constitute a clone for each selected peptide. Genomic DNAs of single-phage clones were then isolated and their nucleotide sequence determined. Finally, individual clones were characterized by quantitative fluorescent microscopy employing a Nikon Eclipse TE-2000U, as described above.

Computationally-designed and characterized short AMP sequences were chosen by data mining from the literature.[44,56] The molecular weight (MW), isoelectronic point (pI), charge and grand average of hydropathy (GRAVY) value parameters for each peptide were calculated using ExPASy Proteomics Server.

Peptide Synthesis

An automated solid-phase peptide synthesizer (CS336X; CS-Bio, Menlo Park, CA, USA) was utilized to synthesize peptides through Fmoc-chemistry. In this approach, modified amino acids with the N-terminus and amino acid side chains protected by the Fmoc group and an appropriate protecting group, respectively, were used. In the reaction vessel, the Wang resin (Novabiochem, West Chester, PA, USA), pre-loaded with a Fmoc-protected first amino acid, was treated with 20% piperidine in DMF to remove the Fmoc group and

monitored by UV-absorbance at 301 nm. The incoming amino acid, separately activated with HBTU (Sigma-Aldrich) in dimethylformamide (DMF), was transferred into the vessel and incubated with the resin for 45 min. After washing the resin with DMF, this protocol was applied for the addition of each of the next amino acids.

Following synthesis, the resulting resin-bound peptides were cleaved and the side-chain de-protected using reagent-K [TFA/thioanisole/H_2O/phenol/ethanedithiol (87.5:5:5:2.5)] and precipitated by cold ether. Crude peptides were purified by RP-HPLC with up to >98% purity obtained (Gemini 10u C18 110A column). The sequence of the peptides was confirmed by mass spectroscopy (MS) using a MALDI-TOF mass spectrometry with reflectron (RETOF-MS) on an Autoflex II (Bruker Daltonics, Billerica, MA, USA). Stock solutions of each peptide at 4 mM were made in sterile, de-ionized water by dissolving the peptides. Subsequent dilutions were accomplished with sterile 1× PBS.

Binding Characterization of Peptides onto the Titanium Alloy Implant Surfaces

Fluorescent microscopy characterization procedure was applied to investigate the binding affinities for both the TiBP and the AMP-conjugated bifunctional chimeric peptides. In this assay, the biotinylated peptide was incubated with pre-cleaned substrates for 3 h at room temperature. Following that, the substrates were washed three times with 1× phosphate-buffered saline (PBS) and the bound peptides were labeled with streptavidin-Alexa Fluor 488 (Molecular Probes, Eugene, OR, USA) by incubation for 15 min in the dark. The substrates were washed with de-ionized water three times and the bound peptides were visualized on the substrate surface by a fluorescent microscope. All measurements were carried out in triplicate independent experiments.

Bacterial Maintenance and Culturing

Three bacteria species—*E. coli* American Type Culture Collection (ATCC) 2592, *S. mutans* ATCC 25175, and *S. epidermidis* ATCC 29886—were used in the present study. All were cultured according to ATCC protocol using the following media: trypticase soy broth (TSB) for *E. coli*, brain heart infusion (BHI) broth for *S. mutans*, and nutrient broth (NB) for *S. epidermidis*. For all three bacterial species, the bacterial pellet obtained from ATCC was rehydrated in 0.5 mL of the above-specified media, and several drops of the suspension were immediately streaked on the relevant solid media. The agar plate was then incubated aerobically at 37°C for 24 h, except in the case of *S. mutans* which was incubated in the presence of a 5% CO_2-supplemented atmosphere. *S. mutans* overnight cultures were made by aseptically transferring a single-colony forming unit into 10 mL of BHI, followed by aerobic incubation at 37°C in the presence of 5% CO_2 for 16 h under static conditions. Overnight cultures of *S. epidermidis* and *E. coli* were made by aseptically transferring a single-colony forming unit into 10 mL of NB or TSB, respectively, followed by aerobic incubation at 37°C with constant agitation (200 rpm) for 16 h.

In-Solution Antimicrobial Activity of Chimeric Peptides

The in-solution antimicrobial activity of the chimeric peptide was analyzed against *S. mutans, S. epidermidis,* and *E. coli* spectrophotometrically. For each bacteria species, solutions of selected AMPs were added into the specified media to reach predetermined final concentrations and inoculated with the bacteria to a final concentration of 10^7 cells/mL. Bacterial growth at 37°C was monitored over the course of 24 h by optical density measurements at 600 nm on a Tecan Safire spectrophotometer. Each experiment contained control samples consisted solely of 10^7 cells/mL of bacteria in the specified media.

Bacterial Adhesion and Quantification on Chimeric Peptide Coated Implant Surfaces

Pre-cleaned titanium substrates were incubated at 37°C under constant agitation (200 rpm) with chimeric peptide solution and removed after 3 h. An aliquot of 1 mL of sterile 1× PBS was then added to each well, agitated by pipetting three times and removed from the well. A second 1-mL aliquot of sterile 1× PBS was added to each well, agitated as before, and removed from the well. Using sterile forceps, each titanium substrate was moved to a clean well that was free of any peptides.

To proceed with bacterial adhesion experiments, overnight cultures of each bacterium were prepared as described above. Bacteria from the overnight cultures were used to inoculate fresh media to a final concentration of 10^7 cells/mL. Cultures were incubated until they reached the mid-log phase as determined by optical density measurement at 600 nm, collected by centrifugation at 2000×*g* for 5 min. The supernatant was decanted and the bacterial pellet was re-suspended in 500 μL of the specified media. This suspension was transferred to a 2-mL centrifuge tube and centrifuged at room temperature at 2000×*g* for 3 min. The supernatant was carefully removed and the bacterial pellet was re-suspended in sterile 1× PBS to a final concentration of 10^8 cells/mL. An aliquot of 1 mL of the 10^8 cells/mL cell suspension was added to each well containing a chimeric peptide-modified titanium substrate, and incubated for 2 h. For the *S. mutans* experiments, incubation was carried out at 37°C in the presence of 5% CO_2 under static conditions; for *S. epidermidis* and *E. coli* experiments, incubation was carried out aerobically at 37°C under constant agitation (200 rpm). After 2 h incubation, the bacterial suspension was removed by aspiration and the surfaces were washed two times

with 1 mL of 1× PBS. Bacterial cells adhered to the titanium substrates were fixed with 500 μL of 2% glutaraldehyde for 30 min, followed by dehydration in a series of increasing gradient of water: alcohol baths, consisting of 50% ethanol for 10 min, 70% ethanol for 10 min, 90% ethanol for 10 min, and a final 1 mL of 100% ethanol. Detection of the bacterial cells was carried out by the addition of 500 μL of 5 μM SYTO9 green fluorescent nucleic acid stain (Invitrogen, Carlsbad, CA) added to each well containing a substrate, protected from light, and incubated for 20 min. Substrates were washed three times with 1 mL of 1× PBS, and each aliquot was agitated by re-pipetting twice. After washing, the substrates were secured onto a clean microscope slide and viewed with a Nikon Eclipse TE2000-U fluorescent microscope. Images were obtained from five random sites of implant surfaces and analyzed for percent surface coverage using MetaMorph (v.6.r6) software.

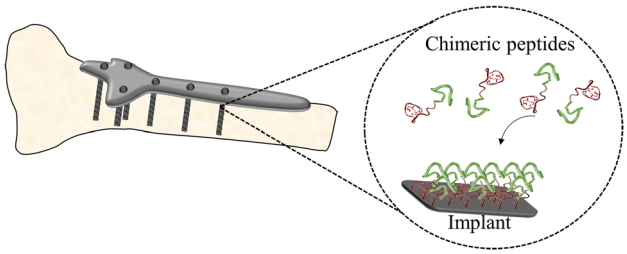

Fig. 1. Schematics of biological self-assembly of chimeric antimicrobial peptide coating of titanium implant surface.

Chimeric Peptide Structure Determination and Structure–Function Analysis

The structure of the peptides was investigated by the fragment insertion method using the Robetta server, followed by energy minimization routing using PyRosetta software.[57–59] Two hundred decoys were energy minimized for each sequence. The lowest energy structure was taken as the best estimate of the structure in solution for the molecular descriptor analysis. All decoys were used for the secondary structure analysis of the length of alpha helix, the length of right-handed alpha-helices and the length of left-handed alpha helices. DSSP[60] was used to calculate the secondary structure based upon three-dimensional atomic coordinates for a peptide structure. Rules were induced by the Modified Learning from the Experience Module (MLEM2) version 2.[61] Only the rules that label all cases in the data more accurately than a rule without conditions are given in the results.

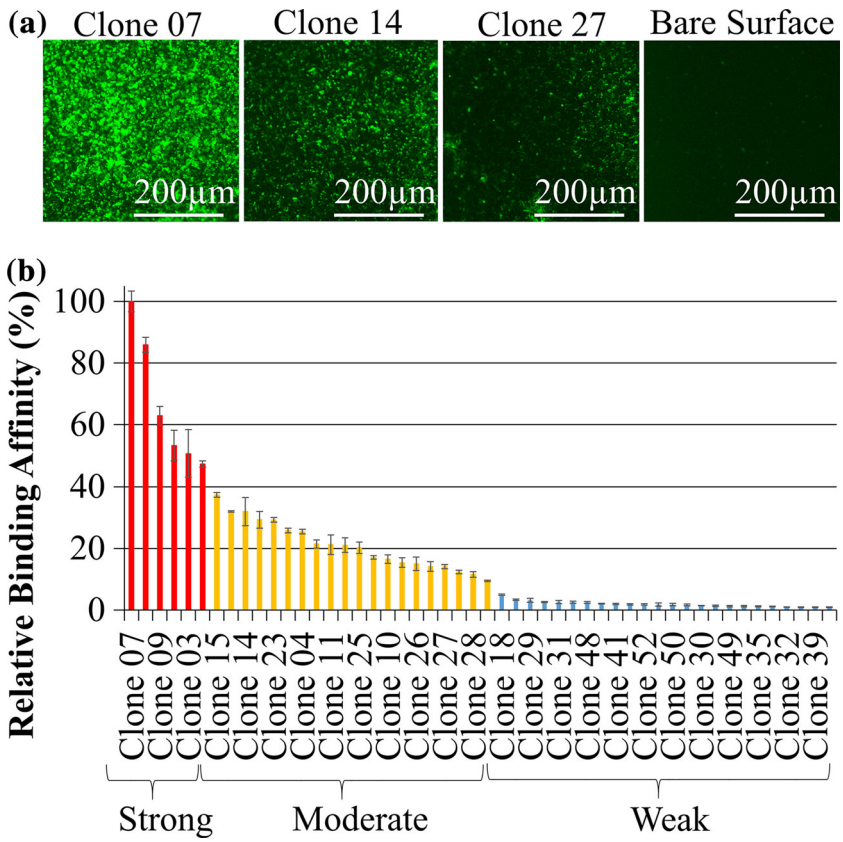

Fig. 2. Phage-bound titanium binding peptides (TiBPs) selected by phage display: (a) examples of FM images of TiBPs with different binding affinities; (b) categorization of the titanium binding phage clones based on relative binding affinity analysis via FM

RESULTS AND DISCUSSION

In this study, we demonstrated the use of chimeric peptides as antimicrobial coating agents on titanium grade V implants (Fig. 1). Bifunctional chimeric peptides, comprising a combinatorially-selected titanium binding and computationally-designed antimicrobial domains, were constructed. Surface-binding characterizations of these peptides were investigated using fluorescent microscopy. Antimicrobial activity of these bifunctional peptides were demonstrated against different pathogens common to implant infections; *S. mutans*, *S. epidermidis*, and *E. coli*. The potential molecular property rules were elaborated for the related sequence- activity relationships of the peptides following their folding patterns in the secondary structures.

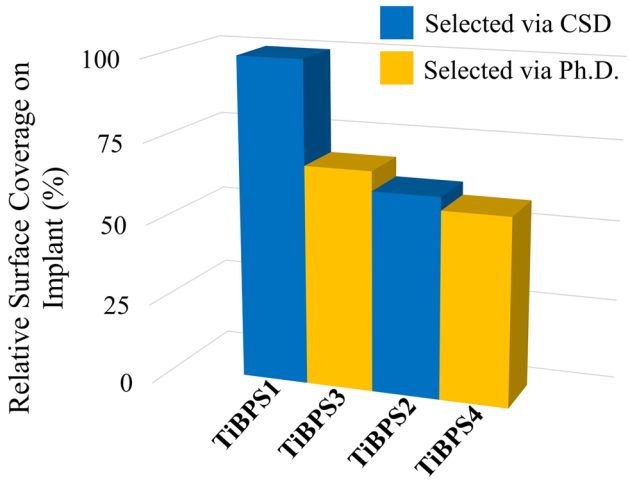

Fig. 3. Relative binding affinities of titanium binding peptides (TiBPs) selected by cell surface display (CSD) and phage display (Ph.D.). Phage-bound TiBPS3 and TiBPS4 are represented in previous figures as Clone 7 and Clone 22, respectively.

Selection and Characterization of Solid Binding Peptides

The phage display technique[55] was applied on titanium grade V powder to select peptides that could serve as potential molecular linkers to tether AMPs on the implant material surfaces. Throughout the selection process, four successive rounds of biopanning were performed, resulting in 50 unique clones, which were subjected to DNA nucleotide sequence determination and analysis. The fluorescent microscopy technique is a semi-quantitative binding assay that was applied to investigate the affinity level among each of the TiBP expressed by individual clones. For this assay, each clone was incubated with titanium grade V powder and then visualized using an anti-M13-specific antibody and fluorophore-labeled secondary antibody. To evaluate the specific surface affinity of individual clones, the bound phage clones expressing titanium binding sequences were visualized as uniformly distributed bright green rods on a dark background of the implant material, as opposed to the wild-type M13 phage, which fail to bind. Based on these results, all the identified peptides were successfully categorized as strong, moderate and weak binders (Fig. 2).

To eliminate the internal bias resulting from the amino acid distribution for each phage display and cell-surface display library, the two strongest peptides selected via phage display were further characterized and compared with TiBP that are previously selected by cell surface display and characterized.[50] Each identified peptide was synthesized with biotin and incubated with titanium implants. After removing the unbound peptides, surface coverage of each peptide were visualized by using fluorophore probes attached via interaction of biotin with streptavidin. Surface coverage ratios as well as the predicted MW, pI, net charge and GRAVY values of synthesized TiBP are depicted in Fig. 3 and Table I.

Table I. The physicochemical properties of the selected titanium binding peptides (TiBP), MW, pI, net charge and the hydropathy values

Peptide name	Sequence	MW (kDa)	pI	Charge	GRAVY score
TiBPS1	RPRENRGRERGL	1495.6	11.82	+3	−2.633
TiBPS2	SRPNGYGGSESS	1197.1	5.72	0	−1.567
TiBPS3	HAYKQPVLSTPF	1387.6	8.60	+1	−0.333

Table II. Minimum inhibitory concentration (MIC) values of AMP-1 and AMP-2 against *E. coli*, *S. epidermidis* and *S. mutans*

Peptide	Sequence	*E. coli* (μg/mL)	*S. epidermidis* (μg/mL)	*S. mutans* (μg/mL)
AMP1	LKLLKKLLKLLKKL	16 (9.45 μM)	8 (4.72 μM)	64 (37.81 μM)
AMP2	KWKRWWWWR	32 (21.08 μM)	1 (0.66 μM)	16 (10.54 μM)

Table III. MW, pI, net charge and the hydropathy of designed chimeric peptides

Peptide name	Sequence	MW (kDa)	pI	Charge	GRAVY score
TiBPS1-AMP1	RPRENRGRERGLGGGLKLLKKLLKLLKKL	3341.1	11.85	+9	−0.890
TiBPS2-AMP1	SRPNGYGGSESSGGGLKLLKKLLKLLKKL	3042.6	10.93	+6	−0.448
TiBPS1-AMP2	RPRENRGRERGLGGGKWKRWWWWR	3166.6	12.13	+7	−2.254
TiBPS3-AMP2	HAYKQPVLSTPFGGGKWKRWWWWR	3058.5	11.17	+5	−1.104

Table IV. Minimum inhibitory concentration (MIC) values of chimeric peptides against *E. coli*, *S. epidermidis* and *S. mutans*

Peptide name	Sequence	*E. coli* (μg/mL)	*S. epidermidis* (μg/mL)	*S. mutans* (μg/mL)
TiBPS1-AMP1	RPRENRGRERGLGGGLKLLKKLLKLLKKL	32 (9.58 μM)	16 (4.78 μM)	512 (153.25 μM)
TiBPS2-AMP1	SRPNGYGGSESSGGGLKLLKKLLKLLKKL	64 (21 μM)	16 (5.23 μM)	1024 (336.5 μM)
TiBPS1-AMP2	RPRENRGRERGLGGGKWKRWWWWR	256 (80.8 μM)	8 (2.52 μM)	256 (80.8 μM)
TiBPS3-AMP2	HAYKQPVLSTPFGGGKWKRWWWWR	512 (167.4 μM)	16 (5.23 μM)	256 (83.7 μM)

Selection and Characterization of Antimicrobial Peptides

Bacteria growth curves in the presence of AMPs with twofold increment concentrations ranging from 1 μg/mL (0.66 μM) to 512 μg/mL (337.92 μM) were analyzed for a 24-h period to determine the minimum inhibition concentration (MIC) value for the each of the bacterial strains common for oral and orthopedic implant infections, i.e., *S. mutans*, *S. epidermidis*, and *E. coli*. As shown in Table II, AMP1 and AMP2 are both effective against three of these organisms, yet each revealed with different MIC values. The MIC values of AMP1 against *E. coli, S. epidermidis*, and *S. mutans* were determined as 9.45 μM, 4.72 μM, and 37.81 μM, respectively. For AMP2, these MIC values against *E. coli, S. epidermidis*, and *S. mutans* were found to be 21.08 μM, 0.66 μM, and 10.54 μM, respectively. These concentrations indicate that AMP1 is more effective against *E. coli* than AMP2, whereas AMP2 prevented *S. mutans* and *S. epidermidis* growth with much lower concentrations than AMP1.

Construction and Characterization of Bifunctional Chimeric Peptides

Bifunctional chimeric peptides having both titanium binding affinity and antimicrobial activity were constructed by coupling the TiBP domain with the AMPs, i.e. either AMP1 or AMP2, in different combinations. In this design, TiBPs were inserted to the C′-terminal ends of the AMPs with a structurally flexible triple glycine (Gly-Gly-Gly) linker sequence to enable the surface display and thus preserve the functionalities of both the TiBP and the AMPs. The amino acid sequences and theoretical parameters, such as MW and pI, for each of the bifunctional peptide are listed in Table III.

Successful design of any bifunctional chimeric peptide requires that the multifunctional activities embedded in the final construct are confirmed. Therefore, the efficiency of the resulting bifunctional chimeric peptide was investigated with respect to titanium binding affinity as well as its antimicrobial activity. To investigate the antimicrobial activity, bifunctional chimeric peptides were tested against strains of *E. coli*, *S. epidermidis*, and *S. mutans* and the resulting MIC values were calculated by spectrophotometrically monitoring bacterial growth in the presence of these bifunctional chimeric peptides. The concentration for each peptide was chosen such that the lowest test concentration was set to the predetermined MIC value of each AMP to ensure that the same number of AMP molecules were present in the solution. The dynamic range was determined using two-fold increment to reach the highest peptide concentrations tested.

As shown in Table IV, among five different bifunctional chimeric peptides, those that were harboring AMP1 as an antimicrobial counterpart, i.e. TiBPS1-AMP1 and TiBPS2-AMP1, showed the most effective antibacterial activity against *E. coli,* at concentrations of 9.58 μM and 21 μM, respectively. Furthermore, compared to the TiBPS2-AMP1, TiBPS1-AMP1 was revealed to be two times more effective in its antimicrobial activity. The attenuation in the antimicrobial efficiency of AMP1 depended on the TiBP to which it is coupled. This outcome can be attributed to differences in the amino acid composition and the sequences of these bifunctional chimeric peptides. In the case of *S. epidermidis*, it was revealed that the TiBPS1-AMP2 is the most effective peptide in solution, being able to prevent bacterial growth at as low as 2.52 μM concentration. In addition, TiBPS1-AMP1, TiBPS2-AMP1 and TiBPS3-AMP2 also showed considerable

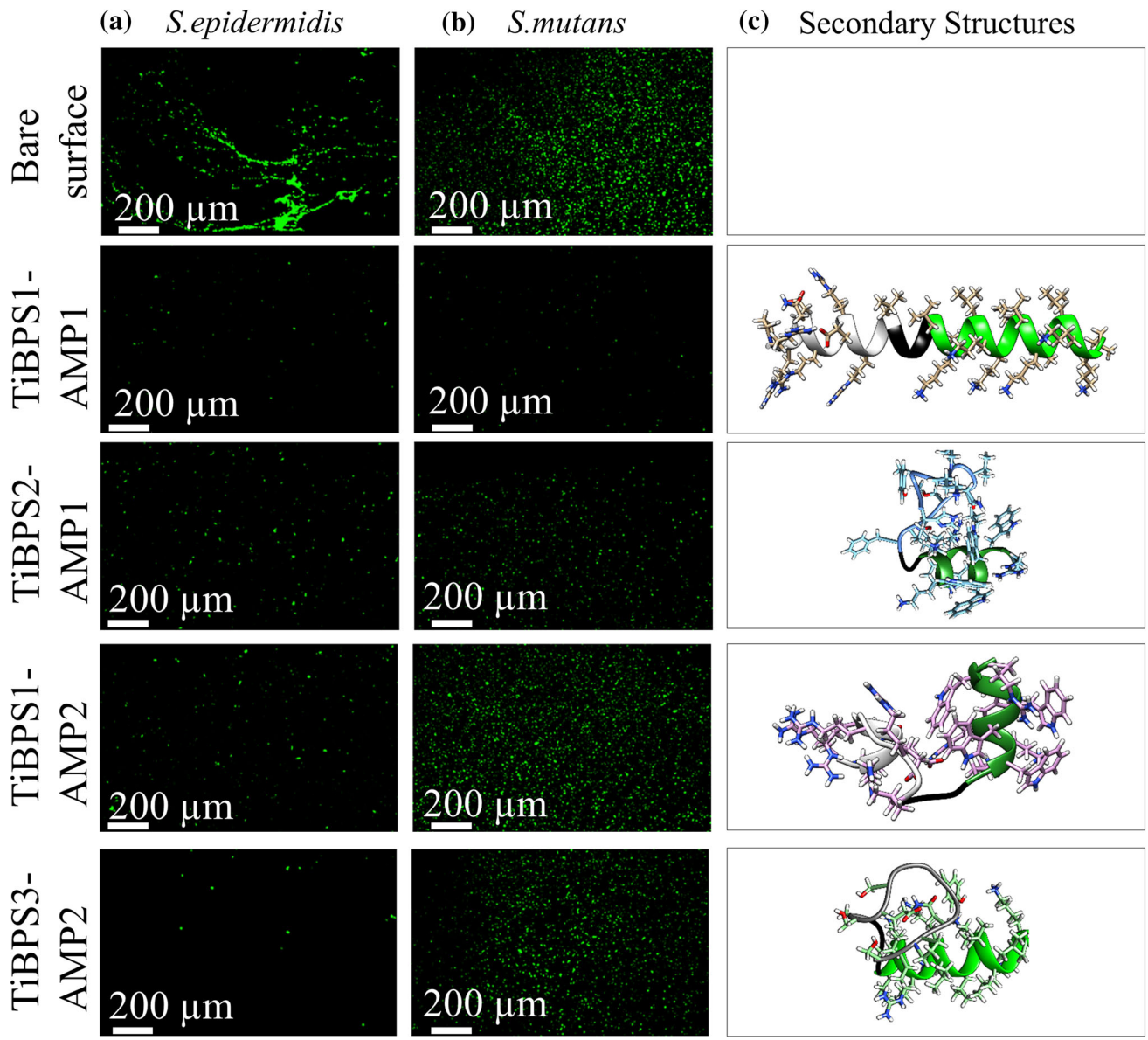

Fig. 4. Bacterial adhesion on peptide-modified titanium implant surfaces against (a) *Staphylococcus epidermidis*, (b) *Streptococcus mutans*, and (c) their predicted secondary structures.

antimicrobial activity, with MIC values of 4.78 μM, 5.23 μM and 5.23 μM, respectively. Interestingly, in contrast to the two-fold reduction in the antimicrobial efficiency of TiBPS2-AMP1 compared to TiBPS1-AMP1 against *E. coli*, these bifunctional peptides did not show the same trend against *S. epidermidis*. This can be attributed to the complex interactions between the bacterial cell membrane and the AMPs during targeting and penetration into the bacterial cell membrane. It also implies that overall antimicrobial activity depends not only on amino acid sequence but also the membrane structure and composition of the targeted microorganism. Also, the hydrophobicity of the AMP, the presence of positively charged residues, amphipatic nature of the peptide, and secondary structure are some of known factors that can affect both the antimicrobial activity and antimicrobial selectivity to specific organisms.

In the case of *S. mutans*, both TiBPS1-AMP2 and TiBPS3-AMP2 showed the highest antimicrobial activity with MIC of 80.8 μM, while for the TiBPS1-AMP1 it was 153.25 μM which again suggests the complex mechanism of antimicrobial action of peptides.

Bacterial Adhesion on Peptide Functionalized Implant Surfaces

Following the determination of the MIC values of each peptide against three different bacterium in solution, the antimicrobial efficacies of these pep-

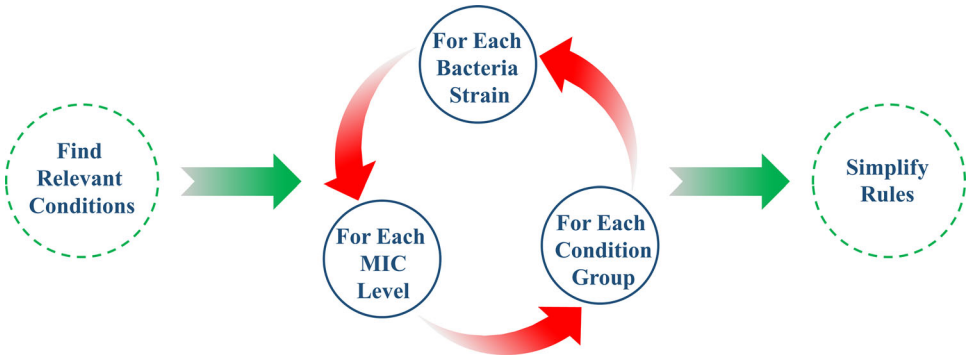

Fig. 5. The algorithm flowchart showing probing rules to describe the antimicrobial functionality of peptides.

Table V. Rules set induced from MW, pI, net charge and the hydropathy for minimum inhibitory concentration (MIC) by molarity

Property	Value interval	Pathogen	MIC interval (μM)	Correct cases/ applicable cases (7 total cases)
pI	9.65–12.13	*E. coli*	9.45–21	3/3
Charge	5.5–9.0	*E. coli*	9.45–21	3/3
GRAVY score	−2.177 to 0.5	*E. coli*	9.45–21	3/3
Molecular weight	1279.5–3341.1	*E. coli*	9.45–21	3/3
pI	10.965–12.13	*E. coli*	167.4–167.6	2/2
Charge	0–5.5	*E. coli*	167.4–167.6	2/2
Molecular weight	3050.55–3341.1	*E. coli*	167.4–167.6	2/2
Charge	3.5–9.0	*S. epidermidis*	4.72–5.23	5/5
GRAVY score	−1.8375 to 0.5	*S. epidermidis*	4.72–5.23	5/5
Molecular weight	1593.95–3341.1	*S. epidermidis*	4.72–5.23	5/5

tides were further characterized on the titanium implant surfaces against *S. mutans*, *S. epidermidis* and *E. coli*.

With this aim, 100 μM of each bifunctional chimeric peptide was incubated for 4 h at 37°C with constant agitation with the sterile titanium implant. The excess peptide was removed by washing surface three times with PBS buffer. Surfaces were incubated with bacteria culture at 10^8 cells/mL for 2 h. After incubation, the cells were fixed and labeled with SYTO 9 dye, which penetrates through the bacterial membranes and stains the cells green. The bacterial binding and antimicrobial efficacy of the peptide-functionalized titanium implant surfaces were analyzed by visualizing under fluorescent microscopy.

As shown in Fig. 4, both the *S. mutans* and *S. epidermidis* adhesion on titanium implants coated with bifunctional chimeric peptides was significantly reduced compared to the bare titanium implant surface. Moreover, in contrast to the in-solution antimicrobial activities discussed above, surfaces coated with TiBPS1-AMP1 and TiBPS2-AMP1 showed similar antimicrobial activities against *S. mutans* and *S. epidermidis*. Compared to AMP2 containing bifunctional chimeric peptides, those harboring AMP1 showed better surface antimicrobial activity against *S. mutans*. These results demonstrate that, with a 30-fold reduction in bacterial adhesion compared to bare surface, the TiBPS1-AMP1 is the most efficient bifunctional chimeric peptide to be utilized for titanium implant surface functionalization against *S. mutans*. On the other hand, against *S. epidermidis*-acquired infections, TiBPS1-AMP1 and TiBPS3-AMP2 would be the better choice for surface functionalization of titanium implants.

Peptide Molecular Property Rules

The AMP sequences tested, AMP1 and AMP2, have complex sequence–activity relationships with bacterial cell membranes that are sensitive to the change between chimeric and single forms. To decipher the sequence-activity relationships of these variants, patterns from multiple sources were considered in deriving two rule sets. Figure 5 provides a diagram of the derivation of each of the two rule sets. The first rule set is based on molecular properties, such as isoelectric point, overall charge, average hydropathy and MW. The second rule set is based on predicted folding patterns of secondary structure in terms of alpha helix length. The peptide AMP efficiency results were divided first by bacteria

Table VI. Rules set induced from lengths of alpha-helices and the chirality of the member residues for minimum inhibitory concentration (MIC) level by molarity

Alpha helix property	Pathogen	MIC interval (μM)	Correct cases/ applicable cases (1400 total cases)
5-a.a.-helix 4-a.a.-right-handed helix	*E. coli*	9.45–21	164/179
5-a.a.-helix 4-a.a.-right-handed helix	*S. epidermidis*	4.72–5.23	164/179
5-a.a.-helix 4-a.a.-right-handed helix	*S. mutans*	10.54–37.81	151/179
8-a.a.-helix 6 or 8-a.a.-right-handed helix	*S. mutans*	336.5	8/11

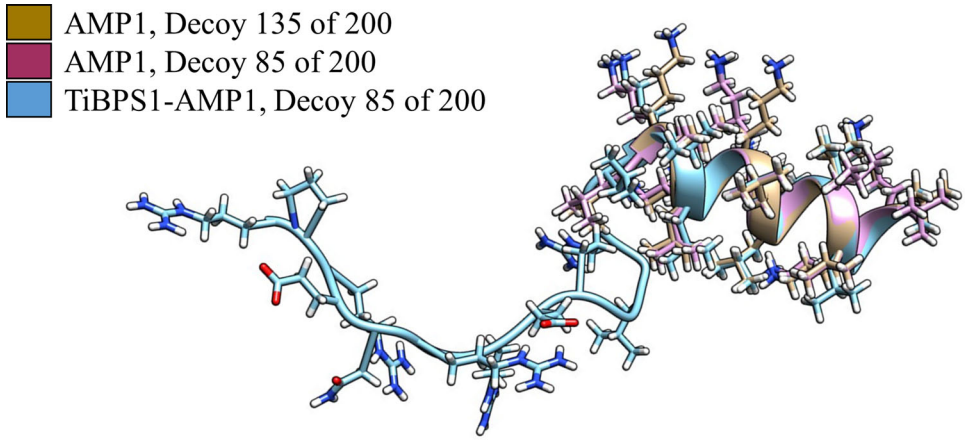

Fig. 6. Structural alignment showing the conserved AMP1 structure in bifunctional chimeric peptides and AMP-only peptides.

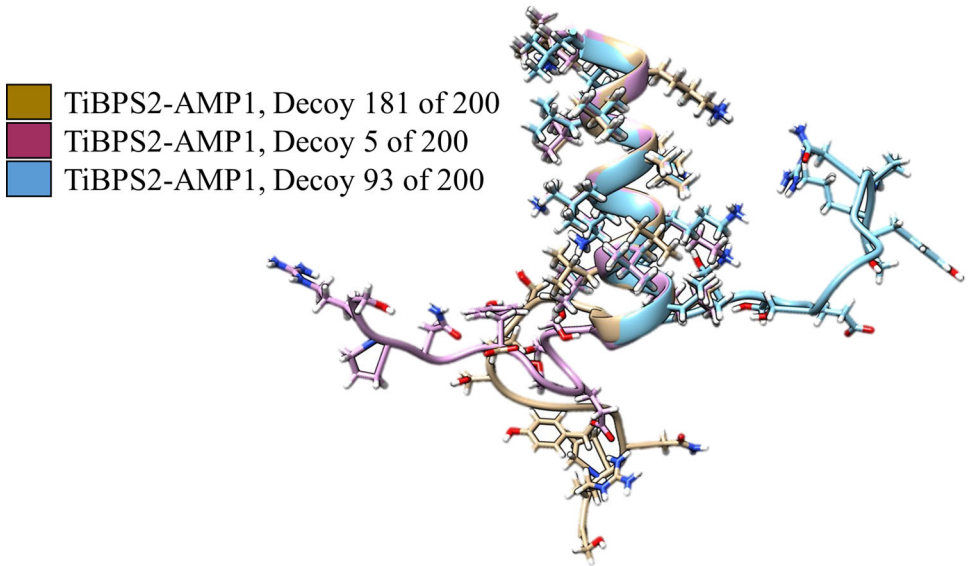

Fig. 7. Structural alignment showing the flexibility of TiBPS2 compared to the secondary structure pattern seen in AMP1 in decoys of TiBPS2-AMP1.

strain. Then, they were subdivided by level of efficiency, such as low, medium and high.

Rules for the most relevant and specific patterns were derived by the rough set theory approach. The rules are simplified if removing a part of a rule does not affect its specificity. A rule is removed if other remaining rules cover the results that it also covers.

For the first rule set, the molecular properties that were the most relevant and specific according to rough set theory to each efficiency level are given by the rules in Table V. The first two columns of the table describe which molecular properties are relevant and specific. The next two columns give the divisions of the data by bacterial strain and by the MIC level. The last column describes how relevant the rule is by stating the number of applicable results to which the rules applies, and describes how specific the rule is by stating the number of those results to which the rule correctly applies.

The first rule set uses the molecular properties as conditions. These rules are certain rules, meaning all of the results that apply are classified correctly. The first two rules imply that to have the lowest observed MIC value of under 21 μM for *E. coli*, the charge of the peptide should be +6 or greater. When the charge is less positive, the MIC level is near 167 μM is expected. The MW range of the first rule indicates that either AMPs in the chimeric or singular form can be effective against *E. coli* at the low MIC value of under 21 μM. The observed constraints for an MIC level for *S. epidermidis* near 5 μM are a positive charge from +4 to +9 with an average hydropathy score of the amino acid residues between −1.84 and 0.5. Negative hydropathy scores relate to hydrophilic amino acids such as arginine. Again, the range of MW shows that the results include an AMP in chimeric form and in an AMP singular form with an MIC efficiency of near 5 μM.

Peptide Structure Function Rules

Peptide structure tendencies may influence the antimicrobial functionality. We performed structural analysis to investigate if there is a trend for their secondary structure tendencies. Figure 4 shows the antimicrobial functionality for four of the bifunctional chimeric sequences against *S. epidermidis* and *S. mutans* and their lowest predicted energy structures. At first glance, comparing the first two peptides with the last two peptides seems to indicate that the longer the alpha helix, the stronger the antimicrobial functionality against these strains.

Here, in order to obtain the lowest energy structure of these chimeric peptides, we performed a further analysis among the hundreds of decoys that are generated to obtain the lowest energy structure that also uncovered trends using the peptide structure tendencies, in addition to the lowest energy structures.

The second rule set (Table VI) was generated to identify predicted secondary structural features that may be responsible for the antimicrobial functionality. Right-handed alpha helices were commonly predicted for the peptides, but no beta-sheet formations were predicted. Left-handed alpha helices are uncommon for systems that use L-Amino acids. The side chains of L-Amino acids would point toward the crowded axis of the helix instead of away. D-Amino acids may form left-handed alpha helices, and for the same reason D-Amino acids generally do not form right-handed helices.[62]

The peptide structure prediction scheme does not explicitly constrain the predicted structures to any particular secondary structure type. The backbone angles were selected from similar fragments in the Protein Databank returned from the Robetta server. A specific conformation of a 5 amino-acid alpha helix in which 4 of the amino acids are predicted to turn toward a right-handed axis seems to be a common predicted secondary structure feature in peptides with MIC values on the order of 10 μM across all three strains. The other identified predicted secondary structural feature is an 8 amino-acid-long alpha-helix associated with an MIC on the order of 100 μM in *S. mutans*. The results from the *E. coli* and *S. epidermidis* were the same because the same sequences were effective against both strains.

Among the predicted structures that the rule induction algorithm identified are many cases of the AMP unit showing the same folded structure in the bifunctional chimeric peptide and the AMP-only sequence were observed. Figure 6 shows decoys of a bifunctional chimeric sequence and two AMP-only sequences that have the same predicted folded structure for the AMP unit. Figure 7 shows three bifunctional chimeric sequence decoys with varied TiBP structure and conserved AMP structure. The AMP secondary structure patterns may be sequence order-specific. If the AMP structure was at the N-terminus, instead of the C-terminus, the TiBP may be more disruptive to its secondary structure patterns. Our results provide an initial scheme to develop design rules for chimeric peptides where their secondary structure predictions could be linked to their observed antimicrobial properties. Combining secondary structure analysis with the experimental evaluations may provide an iterative path for the effective design of engineered peptides to utilize their biological tasks while expanding the functional repertoire with materials-selective biological self-assembly property.

CONCLUSION

We have described a peptide-based implant surface functionalization approach to prevent implant failure due to bacterial infection. Bifunctional chimeric peptides having a specific surface recognition and binding ability, as well as an antimicrobial activity were designed. The implant surface was coated with these chimeric peptides and inoculated with a standard bolus of bacteria culture to test for

bacterial adhesion and/or growth on implant surface. The in-solution activity tests revealed that the functionality of the antimicrobial peptide is conserved when combined in the bifunctional chimeric peptide. The bacterial adhesion studies demonstrated that chimeric peptides coatings provided antimicrobial property for the titanium implants. Collectively, the use of solid binding peptides as molecular recognition units for creating an interface on the implant surface that can be combined with AMPs may enable better control of the tissue–implant interface and thereby leads to modalities that prevent infection and subsequent implant failure. Structure–function relationships used here recognize features putatively leading to the antimicrobial functionality based on individual pathogen data. The analysis of the peptide secondary structures provides guidance for future de novo antimicrobial peptide design specific for diverse surfaces.

By offering single-step and bio-friendly alternatives to the conventional chemical and physical immobilization methods, without the requirement of undesired surface activation processes, solid binding peptides provide new approaches towards merging biological tasks into self-assembly pathways. These short peptides can be the key components to achieve integrated materials–tissue interfaces coupling the large repertoire of biological tasks to the specific sites.

ACKNOWLEDGEMENTS

The authors gratefully acknowledge financial support from National Institute of Health (NIH)—Institute of Arthritis and Musculoskeletal and Skin Diseases (NIAMS), Musculoskeletal Tissue Engineering Section 7R21AR062249-03 and University of Kansas New Faculty General Research Fund (NFGRF) as well as National Institute of Dental and Craniofacial Research Grant DE13045.

REFERENCES

1. S. Bauer, P. Schmuki, K. von der Mark, and J. Park, *Prog. Mater. Sci.* 58, 261 (2013).
2. D. Puleo and A. Nanci, *Biomaterials* 20, 2311 (1999).
3. M. Geetha, A. Singh, R. Asokamani, and A. Gogia, *Prog. Mater. Sci.* 54, 397 (2009).
4. L. Le Guéhennec, A. Soueidan, P. Layrolle, and Y. Amouriq, *Dent. Mater.* 23, 844 (2007).
5. P.H. Pennekamp, J. Gessmann, O. Diedrich, B. Burian, M.A. Wimmer, V.M. Frauchiger, and C.N. Kraft, *J. Orthop. Res.* 24, 531 (2006).
6. J. Costerton, P.S. Stewart, and E. Greenberg, *Science* 284, 1318 (1999).
7. R.A. Weinstein and R.O. Darouiche, *Clin. Infect. Dis.* 33, 1567 (2001).
8. I. Uçkay, P. Hoffmeyer, D. Lew, and D. Pittet, *J. Hosp. Infect.* 84, 5 (2013).
9. V. Antoci Jr, C.S. Adams, J. Parvizi, H.M. Davidson, R.J. Composto, T.A. Freeman, E. Wickstrom, P. Ducheyne, D. Jungkind, and I.M. Shapiro, *Biomaterials* 29, 4684 (2008).
10. M. Kazemzadeh-Narbat, J. Kindrachuk, K. Duan, H. Jenssen, R.E. Hancock, and R. Wang, *Biomaterials* 31, 9519 (2010).
11. C.R. Rathbone, J.D. Cross, K.V. Brown, C.K. Murray, and J.C. Wenke, *J. Orthop. Res.* 29, 1070 (2011).
12. E.M. Hetrick and M.H. Schoenfisch, *Chem. Soc. Rev.* 35, 780 (2006).
13. D. Campoccia, L. Montanaro, P. Speziale, and C.R. Arciola, *Biomaterials* 31, 6363 (2010).
14. G.M. Harbers, K. Emoto, C. Greef, S.W. Metzger, H.N. Woodward, J.J. Mascali, D.W. Grainger, and M.J. Lochhead, *Chem. Mater.* 19, 4405 (2007).
15. A. Shimotoyodome, T. Koudate, H. Kobayashi, J. Nakamura, I. Tokimitsu, T. Hase, T. Inoue, T. Matsukubo, and Y. Takaesu, *Antimicrob. Agents Chemother.* 51, 3634 (2007).
16. Y. An, G. Stuart, S. McDowell, S. McDaniel, Q. Kang, and R. Friedman, *J. Orthop. Res.* 14, 846 (1996).
17. B. Jose, V. Antoci Jr, A.R. Zeiger, E. Wickstrom, and N.J. Hickok, *Chem. Biol.* 12, 1041 (2005).
18. J. Price, A. Tencer, D. Arm, and G. Bohach, *J. Biomed. Mater. Res.* 30, 281 (1996).
19. A. Russell, U. Tattawasart, J.-Y. Maillard, and J. Furr, *Antimicrob. Agents Chemother.* 42, 2151 (1998).
20. D.A. Wininger and R.J. Fass, *Antimicrob. Agents Chemother.* 40, 2675 (1996).
21. L. Harris, L. Mead, E. Müller-Oberländer, and R. Richards, *J. Biomed. Mater. Res. A* 78, 50 (2006).
22. I. Banerjee, R.C. Pangule, and R.S. Kane, *Adv. Mater.* 23, 690 (2011).
23. L. Zhao, P.K. Chu, Y. Zhang, and Z. Wu, *J. Biomed. Mater. Res. B Appl. Biomater.* 91, 470 (2009).
24. B. Gottenbos, H.C. van der Mei, F. Klatter, P. Nieuwenhuis, and H.J. Busscher, *Biomaterials* 23, 1417 (2002).
25. M. Mrksich and G.M. Whitesides, *Annu. Rev. Biophys.* 25, 55 (1996).
26. M. Mohorčič, I. Jerman, M. Zorko, L. Butinar, B. Orel, R. Jerala, and J. Friedrich, *J. Mater. Sci. Mater. Med.* 21, 2775 (2010).
27. J.C. Love, L.A. Estroff, J.K. Kriebel, R.G. Nuzzo, and G.M. Whitesides, *Chem. Rev.* 105, 1103 (2005).
28. L.G. Harris and R.G. Richards, *Injury* 37, S3 (2006).
29. K.A. Brogden, *Nat. Rev. Microbiol.* 3, 238 (2005).
30. A. Giuliani, G. Pirri, and S.F. Nicoletto, *Cent. Eur. J. Biol.* 2, 1 (2007).
31. M. Zasloff, *Nature* 415, 389 (2002).
32. K. Reddy, R. Yedery, and C. Aranha, *Int. J. Antimicrob. Agents* 24, 536 (2004).
33. M. Pasupuleti, A. Schmidtchen, and M. Malmsten, *Crit. Rev. Biotechnol.* 32, 143 (2012).
34. H. Jenssen, P. Hamill, and R.E. Hancock, *Clin. Microbiol. Rev.* 19, 491 (2006).
35. A.B. Ingham and R.J. Moore, *Biotechnol. Appl. Biochem.* 47, 1 (2007).
36. K. Hilpert, M.R. Elliott, R. Volkmer-Engert, P. Henklein, O. Donini, Q. Zhou, D.F. Winkler, and R.E. Hancock, *Chem. Biol.* 13, 1101 (2006).
37. C.D. Fjell, H. Jenssen, K. Hilpert, W.A. Cheung, N. Pante, R.E. Hancock, and A. Cherkasov, *J. Med. Chem.* 52, 2006 (2009).
38. Z. Jiang, A.I. Vasil, J.D. Hale, R.E. Hancock, M.L. Vasil, and R.S. Hodges, *J. Pept. Sci.* 90, 369 (2008).
39. M. Sarikaya, C. Tamerler, A.K.-Y. Jen, K. Schulten, and F. Baneyx, *Nat. Mater.* 2, 577 (2003).
40. D. Campoccia, L. Montanaro, and C.R. Arciola, *Biomaterials* 34, 8533 (2013).
41. P.H. Kwakman, A.A. te Velde, C.M. Vandenbroucke-Grauls, S.J. Van Deventer, and S.A. Zaat, *Antimicrob. Agents Chemother.* 50, 3977 (2006).
42. O. Etienne, C. Picart, C. Taddei, Y. Haikel, J. Dimarcq, P. Schaaf, J. Voegel, J. Ogier, and C. Egles, *Antimicrob. Agents Chemother.* 48, 3662 (2004).
43. P. Appendini and J. Hotchkiss, *J. Appl. Polym. Sci.* 81, 609 (2001).
44. Z. Yan, M.L. Snead, and C. Tamerler, *Nanomedicine* 11, 431 (2015).
45. S.S. Socransky and A.D. Haffajee, *Periodontology 2000* 28, 12 (2002).

46. D. Campoccia, L. Montanaro, and C.R. Arciola, *Biomaterials* 27, 2331 (2006).
47. F. Costa, I.F. Carvalho, R.C. Montelaro, P. Gomes, and M.C.L. Martins, *Acta Biomater.* 7, 1431 (2011).
48. S.R. Meyers, X. Khoo, X. Huang, E.B. Walsh, M.W. Grinstaff, and D.J. Kenan, *Biomaterials* 30, 277 (2009).
49. M. Yoshinari, T. Kato, K. Matsuzaka, T. Hayakawa, and K. Shiba, *Biofouling* 26, 103 (2010).
50. H. Yazici, H. Fong, B. Wilson, E. Oren, F. Amos, H. Zhang, J. Evans, M. Snead, M. Sarikaya, and C. Tamerler, *Acta Biomater.* 9, 5341 (2013).
51. E.E. Oren, C. Tamerler, D. Sahin, M. Hnilova, U.O.S. Seker, M. Sarikaya, and R. Samudrala, *Bioinformatics* 23, 2816 (2007).
52. Z. Lu, K.S. Murray, V. Van Cleave, E.R. LaVallie, M.L. Stahl, and J.M. McCoy, *Nat. Biotechnol.* 13, 366 (1995).
53. C. Tamerler, D. Khatayevich, M. Gungormus, T. Kacar, E.E. Oren, M. Hnilova, and M. Sarikaya, *J. Pept. Sci.* 94, 78 (2010).
54. C. Tamerler and M. Sarikaya, *Acta Biomater.* 3, 289 (2007).
55. U.O.S. Seker, B. Wilson, S. Dincer, I.W. Kim, E.E. Oren, J.S. Evans, C. Tamerler, and M. Sarikaya, *Langmuir* 23, 7895 (2007).
56. C.D. Fjell, H. Jenssen, W.A. Cheung, R.E. Hancock, and A. Cherkasov, *Chem. Biol. Drug Des.* 77, 48 (2011).
57. S. Chaudhury, S. Lyskov, and J.J. Gray, *Bioinformatics* 26, 689 (2010).
58. K.T. Simons, C. Kooperberg, E. Huang, and D. Baker, *J. Mol. Biol.* 268, 209 (1997).
59. P. Bradley, K.M. Misura, and D. Baker, *Science* 309, 1868 (2005).
60. W. Kabsch and C. Sander, *Biopolymers* 22, 2577 (1983).
61. J.W. Grzymala-Busse and W. Rzasa, *Fund. Inform.* 100, 99 (2010).
62. N.E. Shepherd, H.N. Hoang, G. Abbenante, and D.P. Fairlie, *J. Am. Chem. Soc.* 131, 15877 (2009).